



# CHEMISTRY

## A European Journal



### Accepted Article

**Title:** New Size-expanded Fluorescent Thymine Analogue: Synthesis, Characterization, and Application

**Authors:** Shingo Hiroshima, Ji Hoon Han, Hitomi Tsuno, Yusuke Tanigaki, Soyoung Park, and Hiroshi Sugiyama

This manuscript has been accepted after peer review and appears as an Accepted Article online prior to editing, proofing, and formal publication of the final Version of Record (VoR). This work is currently citable by using the Digital Object Identifier (DOI) given below. The VoR will be published online in Early View as soon as possible and may be different to this Accepted Article as a result of editing. Readers should obtain the VoR from the journal website shown below when it is published to ensure accuracy of information. The authors are responsible for the content of this Accepted Article.

**To be cited as:** *Chem. Eur. J.* 10.1002/chem.201900843

**Link to VoR:** <http://dx.doi.org/10.1002/chem.201900843>

Supported by  
**ACES**

WILEY-VCH

## FULL PAPER

# New Size-expanded Fluorescent Thymine Analogue: Synthesis, Characterization, and Application

Shingo Hirashima<sup>†</sup>,<sup>[a]</sup> Ji Hoon Han<sup>†</sup>,<sup>[a]</sup> Hitomi Tsuno,<sup>[a]</sup> Yusuke Tanigaki,<sup>[a]</sup> Soyoung Park<sup>\*</sup>,<sup>[a]</sup> and Hiroshi Sugiyama<sup>\*[a, b]</sup>

**Abstract:** Here we describe the synthesis, photophysical characterization, and application of a new size-expanded thymine nucleoside, <sup>diox</sup>T. <sup>diox</sup>T has desirable qualities as a T surrogate, including excellent quantum yield (0.36) and high environmental sensitivity. When incorporated into single- and double-stranded DNA, <sup>diox</sup>T showed excellent photophysical characteristics including a high quantum yield (average 0.20), and unlike BgQ, demonstrated dependence on neighboring bases without significant destabilization of the duplex. Interestingly, the matched base pair of adenine (A) and <sup>diox</sup>T has the unique property that it exhibits higher fluorescence than mismatched base pairs, and <sup>diox</sup>T has self-quenching effects. As one example of the possible applications of these promising features, we demonstrate single nucleoside polymorphism typing for discrimination of A using <sup>diox</sup>T. The results suggest that <sup>diox</sup>T can be used for a broad range of applications in chemical biology.

## Introduction

Since the first report of the emissive nucleobase 2AP by Stryer in 1969, the development and application of fluorescent nucleic acids have provided very powerful tools to researchers and greatly advanced our understanding of nucleic acid structures, activities, and interactions with other biomolecules.<sup>1–3</sup> Chemical modifications are essential to generate fluorescent nucleobases because of the nonemissive nature of natural nucleobases.<sup>4–7</sup> Development of fluorescent nucleobases is also important to expand the useful artificial genetic alphabet.<sup>8–10</sup> The design and synthesis of fluorescent isomorphous nucleobases are most challenging and important. Chemical modifications are required to retain their structural resemblance to natural nucleobases and allow native Watson–Crick base pairing.<sup>11–13</sup> For instance, Tor and coworkers developed isomorphous fluorescent RNA nucleosides derived from thieno[3,4-d]-pyrimidine and demonstrated their usefulness in various studies including

mechanistic investigations of RNA catalysis and RNA structural analysis.<sup>14–17</sup> We have focused on exploiting the potential of isomorphous emissive DNA analogues based on a thieno[3,4-d]-pyrimidine core.<sup>18–22</sup> Quinazoline structure is also one of the useful fluorescent cores. The quinazoline-derived fluorescent nucleobases have been developed by fusion of electron-rich ring into electron-deficient pyrimidine and used as fluorescent probes.<sup>23–27,54,55</sup> Tor and coworkers devised quinazoline-based fluorescent nucleobases with electron donating amine group at C5 or C7 position, 5- or 7-aminoquinazoline-2,4(1H,3H)-dione, and used for not only developing FRET system with tryptophan in native proteins but also discriminating probe as G mismatched pair.<sup>23,24,55</sup> Luedtke and his coworker synthesized nucleoside analogue based on quinazoline structure with amine group at C6 position, and it was used for various studies such as kinetics of metallo-base pair.<sup>25–27</sup> In this study, we turned our attention to the 1,3-benzodioxole moiety as a heterocyclic core to endow the nucleobases with emissive properties. The 1,3-benzodioxole moiety is a well-known building block found in many naturally occurring compounds that demonstrate anticancer and antioxidant activities.<sup>28–32</sup> Moreover, dioxoloquinazoline derivatives have been investigated because of their biological activities as inhibitors of botulinum neurotoxin serotype A and substrate-competitive inhibitors of G9a (histone lysine methyltransferase).<sup>33,34</sup> To our knowledge, fluorescent DNA nucleoside analogues that include a dioxoloquinazoline core have not been reported.

Here, we synthesized a new size-expanded fluorescent T-mimic deoxyribonucleoside, <sup>diox</sup>T, based on a dioxoloquinazoline core, and explored its biophysical and the photophysical properties. <sup>diox</sup>T showed comparable biophysical properties and displayed notable photophysical characteristics including high brightness ( $\Phi\epsilon$ ) as a fluorescent thymine surrogate. This suggests that <sup>diox</sup>T would be a useful fluorescent probe for chemical biology applications such as a molecular probe for detection of single-nucleotide polymorphisms (SNPs).

## Results and Discussion

### Synthesis of <sup>diox</sup>T nucleoside

The new size-expanded fluorescent thymidine analogue was synthesized using previously reported procedures with minor modifications (Scheme 1).<sup>33,34</sup> Direct oxidative methyl esterification of commercially available 6-nitropiperonal **1** using molecular iodine in methanol produced methyl-6-nitro-1,3-benzodioxole-5-carboxylate **2**. Methyl-6-amino-1,3-benzodioxole-

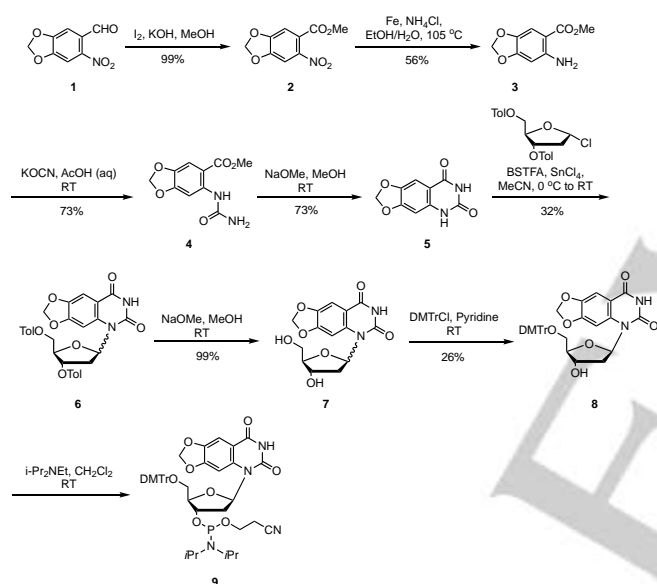
[a] S. Hirashima, Dr. J. H. Han, Dr. S. Park, Prof. Dr. H. Sugiyama  
Department of Chemistry, Graduate School of Science  
Kyoto University, Kitashirakawa-Oiwakecho, Sakyo-ku  
Kyoto 606-8502 (Japan)  
E-mail: oleesy@kuchem.kyoto-u.ac.jp  
hs@kuchem.kyoto-u.ac.jp

[b] Prof. Dr. H. Sugiyama  
Institute for Integrated Cell-Material Science (iCeMS)  
Kyoto University, Yoshida-ushinomiyacho Sakyo-ku  
Kyoto 606-8501 (Japan)

[†] Both authors contributed equally to this work. The authors wish it to be known that the first two authors should be regarded as Joint First Authors.

## FULL PAPER

5-carboxylate **3** was obtained by reduction with Fe powder and  $\text{NH}_4\text{Cl}$ . The fluorescent base moiety **5** was synthesized from **3** by reaction with KOCN, followed by cyclization. Quinazolinone **5** was glycosylated with Hoffer's chlorosugar in the presence of  $\text{SnCl}_4$  and N,O-bis(trimethylsilyl) trifluoroacetamide, and the desired deoxyribonucleosides **6** were obtained in 32% yield as a mixture of  $\alpha$ - and  $\beta$ -anomer. Subsequent toluoyl deprotection of the deoxyribonucleosides **6** with sodium methoxide in methanol produced fluorescent T-mimic deoxyribonucleosides,  $\text{diox}^{\text{T}}$ , at a yield of 99%. By using the conventional method, the 5'-hydroxy group of the nucleoside analogue was protected by a 4,4'-dimethoxytrityl (DMTr) group, and the desired  $\beta$ -anomer was isolated at a yield of 26% by silica column chromatography. The configuration at the C-1 carbon of each anomer was confirmed by 1D and 2D (NOESY) 1H NMR spectroscopy (Figure S1-4). The 3'-hydroxy group of the DMTr protected compound **8** was converted into the phosphoramidite, and the product was used for the automated solid-phase synthesis of oligonucleotides (details in the supporting information).



**Scheme 1.** Synthesis of  $\text{diox}^{\text{T}}$ . Reagents and conditions: (a)  $\text{I}_2$ , KOH, MeOH, 0 °C, 99%; (b) Fe,  $\text{NH}_4\text{Cl}$ , EtOH/ $\text{H}_2\text{O}$ , 105 °C, 56%; (c) KOCN, AcOH (aq.), RT, 73%; (d) NaOMe, MeOH, RT, 68%; (e) 2-Deoxy-3,5-di-O-p-toluoyl- $\alpha$ -D-ribofuranosyl chloride, N,O-Bis(trimethylsilyl)acetamide,  $\text{SnCl}_4$ , MeCN, 0 °C to RT, 32%; (f) NaOMe, MeOH, RT, 99%; (g) DMTrCl, pyridine, RT, 26%; (h) (*i*-Pr) $_2$ NEt, DCM, RT.

### Photophysical properties of $\text{diox}^{\text{T}}$ nucleoside

The basic photophysical properties of  $\text{diox}^{\text{T}}$  mononucleoside were examined in water, methanol, and dioxane (Table 1). In water,  $\text{diox}^{\text{T}}$  showed absorption at 325 nm and fluorescence at 388 nm with high quantum yield (0.36), resulting in very bright fluorescence ( $\Phi_{\text{e}} = 3602 \text{ M}^{-1}\text{cm}^{-1}$ ). This brightness value is higher than previous reported fluorescent thymine/uridine analogues such as  $\text{DMA}^{\text{T}}$  ( $\Phi_{\text{e}} = 87 \text{ M}^{-1}\text{cm}^{-1}$ ), 1PydU and 2PydU ( $\Phi_{\text{e}} \approx 500 \text{ M}^{-1}\text{cm}^{-1}$  in MeOH), bT ( $\Phi_{\text{e}} = 790 \text{ M}^{-1}\text{cm}^{-1}$ ), xT ( $\Phi_{\text{e}} = 1020 \text{ M}^{-1}\text{cm}^{-1}$  in MeOH),  $\text{thd}^{\text{T}}$  ( $\Phi_{\text{e}} = 1984 \text{ M}^{-1}\text{cm}^{-1}$ ) and TPAU ( $\Phi_{\text{e}} = 2200 \text{ M}^{-1}\text{cm}^{-1}$ ).<sup>27,52,53</sup> The absorption and emission spectra of  $\text{diox}^{\text{T}}$  change depending on the solvent. In methanol and dioxane, the lowest

energy absorbance of  $\text{diox}^{\text{T}}$  was slightly blue-shifted to 323 nm and 322 nm, respectively. The emission intensity of  $\text{diox}^{\text{T}}$ , however, dramatically decreased and the emission maxima were significantly shifted toward shorter wavelengths of 377 nm and 361 nm, respectively. Furthermore, the quantum yield of  $\text{diox}^{\text{T}}$  decreased to 0.21 and 0.09, respectively. The corresponding data showed that the lifetime of  $\text{diox}^{\text{T}}$  also tended to decrease in methanol (2.2 ns) and in dioxane (1.0 ns). The Stokes shift of  $\text{diox}^{\text{T}}$  was reduced to  $4435 \text{ cm}^{-1}$  and  $3403 \text{ cm}^{-1}$ , respectively.

**Table 1.** Photophysical characteristic of  $\text{diox}^{\text{T}}$  nucleosides

Solvent	$\lambda_{\text{abs}} / \text{nm}$ ( $\epsilon / 10^3 \text{ M}^{-1}\text{cm}^{-1}$ )	$\lambda_{\text{em}} / \text{nm}$ ( $\Phi$ )	$\Phi_{\text{e}} / \text{M}^{-1}\text{cm}^{-1}$	$\tau / \text{ns}$	Stoke Shift / $\text{cm}^{-1}$
Water	325 (10.90)	388 (0.36)	3602	3.5	4996
MeOH	323 (7.23)	377 (0.21)	1519	2.2	4435
Dioxane	322 (6.93)	361 (0.09)	624	1.0	3403

These results suggest that the photophysical properties of  $\text{diox}^{\text{T}}$  are affected by solvent polarity, indicating that there is a charge transfer in the excited state of  $\text{diox}^{\text{T}}$  compared with its ground state.

### Matched/mismatched base pairing of $\text{diox}^{\text{T}}$ nucleobase inside DNA

To evaluate the biophysical properties of oligonucleotides containing  $\text{diox}^{\text{T}}$  as a dT analogue, we used automated solid-phase synthesis to produce the 18-mer DNA oligonucleotide 5'-CGTCCGTCXTACGCACGC-3', where X =  $\text{diox}^{\text{T}}$ . We also prepared complementary strands containing bases matched or mismatched with  $\text{diox}^{\text{T}}$  and the corresponding natural DNA duplexes containing T. As expected, in thermal denaturation experiments the matched duplex ( $\text{diox}^{\text{T}}$  with A) showed higher thermal stability ( $T_m = 67.2 \text{ }^\circ\text{C}$ ) than did mismatched duplexes containing T, G, and C, indicating that  $\text{diox}^{\text{T}}$  can form a Watson-Crick base pair with A (Figure 1A and 1B). In addition, circular dichroic (CD) spectra of oligomers containing  $\text{diox}^{\text{T}}$  matched with A showed the shape of typical B-form DNA (Figure S8). Therefore, this thermal stability, base pairing selectivity, and CD spectroscopy suggest that  $\text{diox}^{\text{T}}$  can replace native T base without significantly perturbing the DNA structure. Interestingly, as compared with natural base T,  $\text{diox}^{\text{T}}$  shows the higher thermal stability upon mismatched base pairing including abasic (AP) site. Duplex containing  $\text{diox}^{\text{T}}$  and opposite AP site displays significantly higher melting temperature than that of natural T ( $\Delta T_m = 5 \text{ }^\circ\text{C}$ ). Mismatched base pair with C or T show the slightly increased thermal stability around 2 °C. This high  $T_m$  of  $\text{diox}^{\text{T}}$  could be attributed to the increase stacking interactions by expanded aromatic structure of  $\text{diox}^{\text{T}}$  in comparison to that of natural T base. In contrast, thermal stability of  $\text{diox}^{\text{T}}$  mismatched pairing with G is similar to the result from natural T probably due to G:T wobble base pairing (Figure S16). To confirm the fluorescence changes for matched and mismatched oligomers, we measured the steady-state fluorescence. Interestingly, the fluorescence spectra revealed that  $\text{diox}^{\text{T}}$  matched with A had higher fluorescence intensity than did  $\text{diox}^{\text{T}}$  mismatched with G, C, T, and dS (Figure 1C). The fluorescence intensity of  $\text{diox}^{\text{T}}$  located at an AP site was similar to that of a mismatched base pair and lower than that of a matched base pair, suggesting that, consistent with its  $T_m$ ,  $\text{diox}^{\text{T}}$  is strongly bound in the duplex by  $\pi$ - $\pi$  stacking interactions. Furthermore, the lower fluorescence produced by  $\text{diox}^{\text{T}}$  with G and

## FULL PAPER

C as counter bases compared with dS (AP site) may be caused by fluorescence quenching from G, as discussed below.

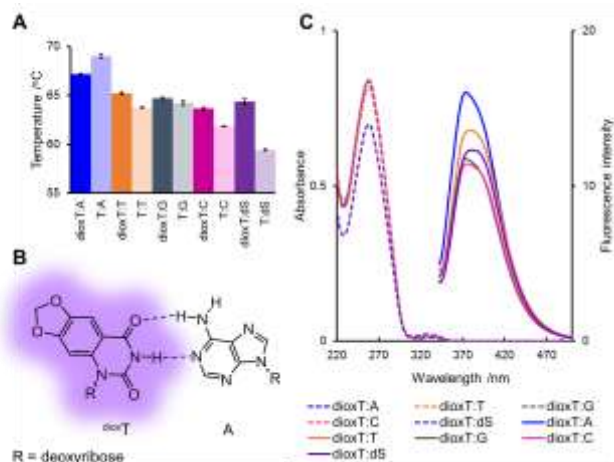


**Figure 1.** Matched/mismatched base pairs with  $dioxT$ . (A) Histogram for the comparison of  $T_m$  values. (B)  $dioxT$  with Watson–Crick base pairing with A. (C) Absorbance (dashed lines) and fluorescence properties (solid lines) of ODN1 hybridized with complementary strands containing matched or mismatched bases. Fluorescence spectra were measured at an excitation of 328 nm. All samples contained 2.5  $\mu$ M of each oligonucleotide strand, 20 mM Na cacodylate (pH 7.0) and 100 mM NaCl. dS indicates 5'-O-dimethoxytrityl-1',2'-dideoxyribose-3'-[(2-cyanoethyl)-(N,N-diisopropyl)]-phosphoramidite.

#### $dioxT$ nucleobase affected by neighboring bases inside DNA

In general, the stability of a duplex containing an artificial nucleobase is strongly affected by its neighboring bases. To investigate the effect of  $dioxT$  incorporated into double-stranded DNA, we measured the  $T_m$  for  $dioxT$  associated with all possible neighboring bases (Table 2). The modified duplex containing  $dioxT$  had a slightly lower  $T_m$  (average 1.9 °C) than the unmodified duplex. Interestingly, sequences in which  $dioxT$  was flanked by two purine bases (PuPu), a pyrimidine and a purine base (PyPu), a purine and a pyrimidine base (PuPy), and two pyrimidine bases (PyPy) all showed similar thermal stability (average 1.4–2.5 °C). This may be attributable to the good integration of  $dioxT$  because

**Table 2.** Thermal stability of  $dioxT$  effected by neighboring bases

Type of nucleobases <sup>a</sup>	Sequence name <sup>b</sup>	$T_m^c$ (°C)	$T_m^d$ (°C)	$\Delta T_m$ (°C)
PuPu	AA	65.3 ± 0.2	67.1 ± 0.03	-1.7 ± 0.1
	AG	67.4 ± 0.4	70.0 ± 0.1	-2.5 ± 0.2
	GA	67.9 ± 0.3	70.3 ± 0.1	-2.4 ± 0.2
	GG	69.8 ± 0.5	73.2 ± 0.1	-3.7 ± 0.3
PyPy	TT	65.7 ± 0.3	68.5 ± 0.2	-2.6 ± 0.2
	TC	69.7 ± 0.1	71.1 ± 0.1	-1.4 ± 0.1
	CT	67.7 ± 0.2	69.2 ± 0.1	-1.5 ± 0.1
	CC	70.6 ± 0.5	73.3 ± 0.2	-2.6 ± 0.3
PuPy	AT	65.4 ± 0.4	66.2 ± 0.2	-0.9 ± 0.2
	AC	68.8 ± 0.6	70.4 ± 0.1	-1.4 ± 0.3
	GT	68.5 ± 0.1	70.3 ± 0.1	-1.7 ± 0.1
	GC	71.7 ± 0.1	73.3 ± 0.1	-1.5 ± 0.1
PyPu	TA	66.1 ± 0.4	68.3 ± 0.2	-1.9 ± 0.2
	TG	69.4 ± 0.2	71.4 ± 0.2	-1.9 ± 0.1
	CA	67.9 ± 0.2	70.2 ± 0.1	-2.2 ± 0.1
	CG	71.1 ± 0.1	72.9 ± 0.2	-1.7 ± 0.1

<sup>a</sup>Type of nucleobase indicates purine (Pu) and pyrimidine (Py) bases. <sup>b</sup>NN denotes sequences named for the neighboring bases surrounding  $dioxT$ . <sup>c</sup>Modified sequence containing  $dioxT$ . <sup>d</sup>Unmodified sequence containing T. All

duplexes were hybridized with matched complementary strand. All samples contained 2.5  $\mu$ M of each oligonucleotide strand, 20 mM Na cacodylate (pH 7.0) and 100 mM NaCl.  $T_m$  experiments were performed in triplicate.

of strong stacking interactions between neighboring bases, even though the  $T_m$  is a little lower than that of the native duplex because of electronic repulsion between the phosphate group and dioxole ring of  $dioxT$  (Figure S10). Duplexes with AT as the neighboring nucleobases showed the highest thermal stability, whereas those with GG showed the lowest thermal stability. As a result, duplexes containing  $dioxT$  demonstrated better thermal stability than the previously reported ring-fused fluorescent nucleobase BgQ.<sup>35</sup>

It is generally known that fluorescent nucleobases are strongly influenced by their nearest-neighbor bases.<sup>36–39</sup> To select suitable sequences for the application, the characteristics of  $dioxT$ -containing single- and double-stranded DNA (5'-CGTCCGTNXNACGCACGC-3', where X =  $dioxT$ , Table 3 and S1) were investigated. The average wavelengths of the absorption maxima of single- and double-stranded DNA containing  $dioxT$  were 325 nm and 327 nm, respectively. Such a red shift of the absorption maximum is typically caused by stacking interactions resulting from the formation of a duplex structure. Consistent with its geometrical characteristics, the emission maximum of  $dioxT$  within double-stranded DNA was slightly blue-shifted compared with that within single-stranded DNA (388 nm and 379 nm, respectively), suggesting that  $dioxT$  located within double-stranded DNA is less polar than that in single-stranded DNA.<sup>49</sup> Despite this, the quantum yields for both single- and double-stranded DNA decreased significantly when G was located next to  $dioxT$ . This quenching effect can be explained by the electron transfer from G. We calculated the order of the highest-occupied molecular orbital (HOMO) energy of each nucleobase as  $G > dioxT > A > C > T$ , which supports the concept that quenching was the result of electron transfer from G (Figure S11). In single-stranded DNA, combinations of  $dioxT$  with A, T, and C, but not G, as neighboring bases showed good quantum yields (0.09–0.23). In double-stranded DNA, all combinations of neighboring base sets containing C (in the 5' position), i.e., CA, CT, CG, and CC, showed higher quenching compared with single-stranded DNA. Both stronger stacking interactions upon formation of double-stranded DNA and electron transfer from neighboring Gs paired with C may have contributed to this quenching phenomenon. Interestingly, neighboring base sets containing A and T showed an average 1.5 times higher quantum yield upon hybridization of double-stranded DNA compared with that in single-stranded DNA. The comparable thermal stability, hypochromic effect, and red shift of  $dioxT$  in duplex DNA indicate that  $dioxT$  is well stacked between base pairs and does not flip to the outside of the duplex. Furthermore, the overall brightness of  $dioxT$  in ds DNA shows average  $622 \text{ M}^{-1}\text{cm}^{-1}$  (Table S2), and this value is significantly higher than that of bT (average  $\Phi_\epsilon = 28 \text{ M}^{-1}\text{cm}^{-1}$  in duplex) and  $^{th}dT$  ( $\Phi_\epsilon = 90 \text{ M}^{-1}\text{cm}^{-1}$  in ds DNA, 5'-GCGCGA<sup>th</sup>dTA<sup>th</sup>dTA<sup>th</sup>dTAGGAGC-3'),<sup>20,52</sup> but less than fluorescent adenine and guanine analogues such as tC<sup>o</sup> ( $\Phi_\epsilon = 2000 \text{ M}^{-1}\text{cm}^{-1}$ ) and 6MI ( $\Phi_\epsilon = 1700 \text{ M}^{-1}\text{cm}^{-1}$ ).<sup>53</sup>

To determine the emissive properties of  $dioxT$ , we analyzed the HOMO and the lowest-unoccupied molecular orbital (LUMO) (Figure S9). The charge density of the HOMO of  $dioxT$  showed that the orbitals populated were those of two oxygens and the CH<sub>2</sub> group of the dioxole ring as well as those of the carbon atoms in the benzene ring. LUMO analysis showed that the orbitals were located in the carbon atoms of the benzene ring and the ketone group at the C4 position of the thymine scaffold, with a minor population on the methoxy group of the dioxole ring. This suggests that substantial charge transfer could occur from the dioxole ring to the benzene ring fused with the thymine moiety.

## FULL PAPER

**Table 3.** Photophysical properties of single and double stranded DNA containing  $\text{dioxT}^a$ 

Sequence name	ssDNA				dsDNA				
	NN <sup>b</sup>	$\lambda_{\text{Abs}}$ (nm)	$\lambda_{\text{Em}}$ (nm)	$\Phi_f$ <sup>c</sup>	$\langle \tau \rangle$ (ns) <sup>d</sup>	$\lambda_{\text{Abs}}$ (nm)	$\lambda_{\text{Em}}$ (nm)	$\Phi_f$ <sup>c</sup>	$\langle \tau \rangle$ (ns) <sup>d</sup>
AA		322	388	0.15	3.43	327	377	0.20	3.11
AC		323	392	0.23	3.50	325	377	0.13	2.26
AG		323	388	0.02	2.01	328	379	0.01	0.97
AT		330	387	0.12	3.15	325	377	0.19	3.13
CA		322	388	0.12	2.31	327	380	0.04	1.01
CC		325	386	0.13	2.30	327	377	0.05	1.57
CG		327	389	0.01	1.83	326	377	0.01	0.40
CT		327	384	0.11	2.12	327	375	0.03	1.13
GA		321	393	0.01	2.37	327	387	0.01	2.25
GC		324	390	0.02	2.76	330	381	< 0.01	1.95
GG		325	385	< 0.01	3.20	324	381	0.05	3.18
GT		326	390	0.01	2.34	326	383	< 0.01	1.95
TA		325	387	0.11	2.04	330	378	0.19	2.48
TC		328	385	0.13	2.18	328	375	0.12	1.31
TG		322	389	0.01	1.58	330	383	0.01	0.61
TT		326	385	0.09	1.88	328	374	0.17	2.36

<sup>a</sup> Measurements were performed at room temperature. All duplexes were hybridized with matched complementary strand. All samples contained 20 mM Na cacodylate (pH 7.0) and 100 mM NaCl. <sup>b</sup> NN denotes the sequences named for the neighboring bases surrounding  $\text{dioxT}$ . <sup>c,d</sup> For the measurement of lifetime and quantum yield, all samples contained 5  $\mu\text{M}$  of each oligonucleotide strand. Quantum yield measurements were performed in duplicate and the average value is shown.

In previous reports, some fluorescent nucleobases such as  $\text{DMA}^{\text{T}}$ , 2PyG, 4AP, and 8-DEA-tC showed enhanced fluorescence depending on their location in double-stranded DNA, a unique phenomenon that could be explained by a charge-separated excited state.<sup>40–42</sup> Therefore, the intramolecular charge transfer of  $\text{dioxT}$  might contribute to the enhancement of quantum yield upon the formation of double-stranded DNA. Both this enhancement and the high quantum yield of  $\text{dioxT}$ -containing DNA duplexes will allow the development of many useful tools.

To utilize the advantages of the photophysical properties of enhanced quantum yield upon conversion from single-stranded DNA to double-stranded DNA and the strong fluorescence of Watson–Crick base pairing with A, we evaluated the use of  $\text{dioxT}$  for SNP typing. This technique has received attention because SNPs can act as biological markers of disease-causing genes and predict individual responses to certain drugs.<sup>43–45</sup> To confirm the ability to discriminate SNPs using  $\text{dioxT}$ , we measured steady-state fluorescence spectra and visualized samples by photographing them under UV (302 nm) irradiation (Figure 2A). We selected sequences containing  $\text{dioxT}$  flanked by AT and TA from combinations of neighboring bases including A and T (AA, AT, TA, and TT). In both instances, fluorescence of  $\text{dioxT}$  was enhanced by approximately twofold upon hybridization with A compared with that in single-stranded DNA (Figure 2B and 2C). Furthermore, as we expected, a DNA duplex containing  $\text{dioxT}$  had higher fluorescence intensity than did other duplexes in which  $\text{dioxT}$  was mismatched with T, C, or G, while  $\text{dioxT}$  mismatched with G as a counter base showed the lowest fluorescence intensity. The photographs of samples under UV irradiation confirmed the ability to discriminate A using changes in  $\text{dioxT}$  fluorescence (Figure 2D and 2E). Interestingly, different base discriminating ability was observed depending on the incorporation position of

electron donating groups on quinazoline ring. The present result is very similar with  $\text{DMA}^{\text{T}}$ ,<sup>27</sup> in which amino group attached at C6 position, while quinazoline-based nucleobase with amino group at C7 position doesn't show enhanced fluorescence upon hybridizing with A.<sup>24</sup> Although several fluorescent nucleobases have been exploited for SNP typing,<sup>46–48</sup> there are very few examples of the use of fluorescent isomorphous T analogues. This result suggests that  $\text{dioxT}$  can be utilized as a SNP typing detector for A.<sup>24–27</sup>

#### Multiple $\text{dioxT}$ nucleobases inside DNA

To investigate  $\text{dioxT}$  further, we also characterized the photophysical behaviors of DNA oligonucleotides containing multiple  $\text{dioxT}$ s (Figure 3A). We prepared DNA oligomers containing three adjoining or alternating  $\text{dioxT}$ s in the center positions, and measured the absorbance and fluorescence spectra of single- and double-stranded DNA (Figure 3B and 3C). Compared with the absorbance of duplex ODN1:ODN1', duplex ODN2:ODN2' showed a blue-shifted band. This might be caused by the degree of alignment of the transition dipole moment of adjoining  $\text{dioxT}$ s.<sup>50,51</sup> For the single-stranded DNAs, ODN1 showed approximately 2.3-fold lower fluorescence intensity than did ODN2. After hybridization with their complementary strands, the increase in fluorescence intensity of duplex ODN1:ODN1' was about 1.5-fold lower than that of ODN2:2', suggesting that multiple  $\text{dioxT}$ s might interact and reduce fluorescence intensity by self-quenching. This hypothesis is supported by the observation that three adjoining  $\text{dioxT}$ s had similar intensity to a single  $\text{dioxT}$  (Figure S12). As indicated in Table 3, it is not surprising that duplex formation by both oligonucleotides resulted in enhanced fluorescence because of the unique properties of  $\text{dioxT}$ . Upon

## FULL PAPER

hybridization of single-stranded to double-stranded

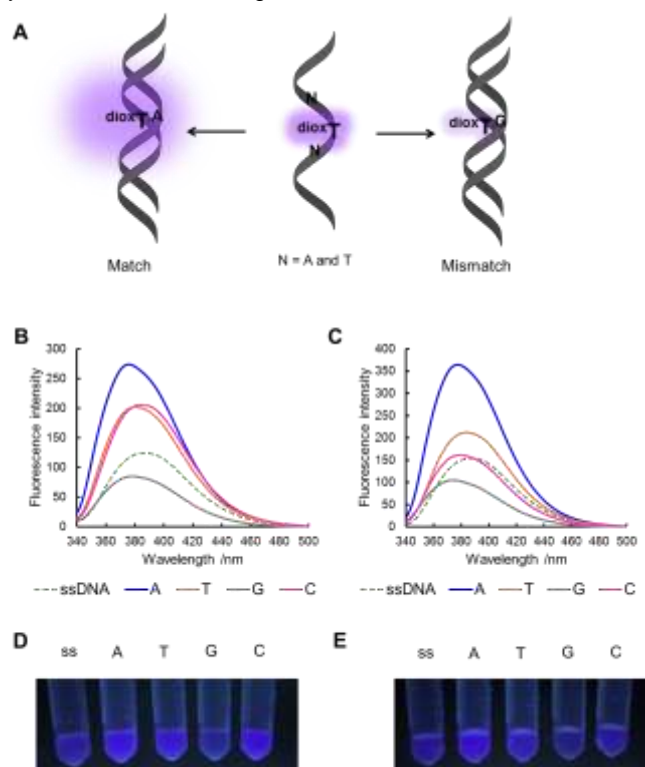


**Figure 2.** Application of  $\text{dioxT}$  for single nucleotide polymorphism (SNP) typing. (A) Schematic illustration of the SNP typing method using oligomers containing  $\text{dioxT}$  (B) Fluorescence spectra of single- and double-stranded DNA containing  $\text{dioxT}$  flanked by bases TA at an excitation of 328 nm. (C) Fluorescence spectra of single- and double-stranded DNA containing  $\text{dioxT}$  flanked by bases AT at an excitation of 330 nm. (D) and (E) Fluorescence images for sequences with the bases opposite  $\text{dioxT}$  flanked by TA and AT under UV (302 nm) irradiation. ss denotes single-stranded DNA. All samples contained 10  $\mu\text{M}$  of each oligomer, 20 mM Na cacodylate (pH 7.0), and 100 mM NaCl.

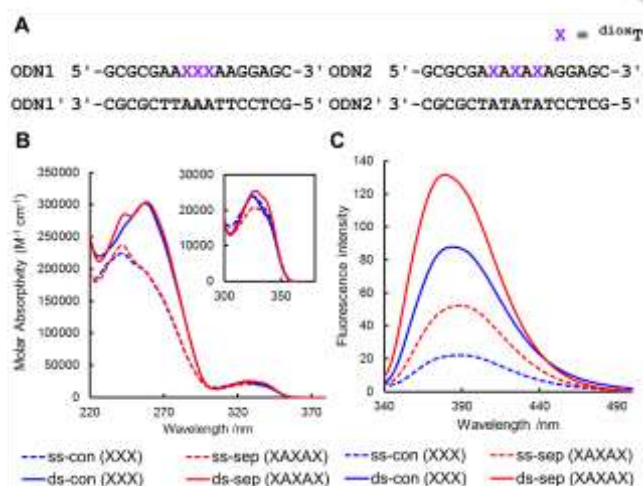


**Figure 3.** Self-quenching analysis of  $\text{dioxT}$ . (A) Oligonucleotide sequence containing  $\text{dioxT}$ . X denotes  $\text{dioxT}$  (B) Absorbance of single- and double-stranded DNA containing  $\text{dioxTs}$  located at adjoining and alternating positions. (C) Fluorescence of single- and double-stranded DNA containing three  $\text{dioxTs}$

located at adjoining and alternating positions. The excitation wavelength is 328 nm. All samples contained 2.5  $\mu\text{M}$  of each oligomer, 20 mM Na cacodylate (pH 7.0) and 100 mM NaCl. ss- and ds- indicate single- and double-stranded DNA, respectively. "con (XXX)" denotes the oligomer containing three adjoining  $\text{dioxTs}$ , ODN1, and "sep (XAXAX)" denotes the oligomer containing three alternating  $\text{dioxTs}$ , ODN2.

DNA, the fluorescence of ODN1:1 was enhanced fourfold, whereas that of ODN2:2' increased 2.5 times and the fluorescence of DNA containing three adjoining  $\text{dioxTs}$  increased significantly more than that of DNA containing a single  $\text{dioxT}$ . These results indicate that three adjoining  $\text{dioxTs}$  may be spatially separated by a  $\text{dioxT}$ - $\text{dioxT}$  interaction resulting from hydrogen bonding with the counter base upon duplex formation. In addition, DNA duplexes containing three adjoining  $\text{dioxTs}$  had higher thermal stability by around 3.5  $^{\circ}\text{C}$  compared with those of duplexes containing three alternating  $\text{dioxTs}$  (data not shown). This higher stability is attributable to the strong stacking interactions of  $\text{dioxT}$  itself. This property may be useful to the development of versatile tools to probe conformational changes in nucleic acids and of molecular beacons based on the self-quenching characteristics of one fluorophore.

## Conclusions

In conclusion, we have synthesized a new size-expanded fluorescent T-mimic deoxynucleoside,  $\text{dioxT}$ , and demonstrated its biophysical and photophysical properties as a T surrogate.  $\text{dioxT}$  showed an excellent quantum yield (0.36) in water and its fluorescence intensity was changeable depending on environmental factors such as solvent polarity. When  $\text{dioxT}$  was incorporated into DNA, it was noteworthy that the fluorescence of the Watson-Crick pairing of  $\text{dioxT}$  and A was higher than that of mismatched pairs. Furthermore,  $\text{dioxT}$  flanked by combinations of neighboring bases such as AA, AT, TA, and TT showed enhanced fluorescence with a significant quantum yield upon duplex formation. These promising features suggest that  $\text{dioxT}$  may be a useful tool for applications in chemical biology such as molecular beacon assays, monitoring of structural changes in nucleic acids and molecular imaging of living cells. We demonstrated one example of the possible applications, visual discrimination of SNPs for typing, by successfully distinguishing samples containing a  $\text{dioxT}$ -A matched pair using the naked eye. In addition, we identified a significant self-quenching effect with DNAs containing multiple  $\text{dioxTs}$ . Investigation of further applications of  $\text{dioxT}$  is underway in our laboratory.

## Experimental Section

Materials used for synthesis of  $\text{dioxdT}$

2-Cyanoethyl N,N-diisopropylchloro phosphoramidite and dimethoxytrityl chloride were received from Wako Chemicals and used without further purification. N,O-bis(trimethylsilyl)trifluoroacetamide was received from TCI. All other chemicals and solvents were purchased from Sigma-Aldrich Chemicals Co., Wako Pure Chemical Ind. Ltd., TCI, and used without further purification. 2-Deoxy-3,5-di-O-p-toluoyl- $\alpha$ -D-ribofuranosyl chloride was prepared by following the literature procedure.<sup>56</sup> Synthetic oligonucleotides were obtained from Sigma Genosys. Water was

## FULL PAPER

deionized (specific resistance of > 18.0 MΩ cm at 25 °C) by a Milli-Q system (Millipore Corp.)

## Absorption and UV-melting measurement

Melting temperatures were determined by measuring changes in absorbance at 260 nm as a function of temperature using a JASCO V-650 UV/VIS spectrophotometer. JASCO PAC-743R equipped with a high performance temperature controller and micro auto eight-cell holder. Absorbance was recorded in the forward and reverse direction at temperatures from 5 to 95 °C at a rate of 1 °C/min. The melting samples were denatured at 95 °C for 3 min and annealed slowly to RT then stored at 5 °C until experiments were initiated. All melting samples were prepared in a total volume of 110 μl containing 2.5 μM of each strand oligonucleotide, 20 mM Na cacodylate (pH 7.0) and 100 mM NaCl. Synthetic oligo nucleotides were obtained from Sigma-Aldrich Chemicals Co.

## Steady state fluorescence measurement

Fluorescence measurements were conducted using fluorescence cells with a 0.5-cm path length on a JASCO FP-6300 Spectrofluorometer equipped with a JASCO EHC-573 temperature controller. The emission spectra were recorded from 350 nm to 600 nm with an excitation wavelength at 325 nm.

## Time resolved fluorescence measurement

Fluorescence decay curves were collected on a HORIBA Fluorocube 3000U-SHK using an LED laser source for excitation. All samples were excited at 317 nm and the fluorescent decay was observed at 388 nm. TAC range was 100 ns and repetition rate was 1 MHz.

Quantum yields of <sup>diox</sup>T monomer

Quantum yields were measured with HAMAMATSU Absolute PL Quantum Yield spectrometer, Quantaurus-QY C11347-11 (Hamamatsu Photonics, Japan), which is a fluorescence spectrophotometer equipped with an integrating sphere for compensating the effects of polarization and refractive index. The reported quantum yields were calculated by using the attached measurement software as shown in the web site

(<http://www.hamamatsu.com/jp/en/product/category/5001/5009/5033/C11347-11/index.html>).

## CD Spectroscopy

CD spectra of 5 μM oligonucleotide solutions collected in 0.5-nm steps from 320 to 220 nm were measured using JASCO J-805LST Spectrometer in a 1 cm quartz cuvette at 5 °C. Each spectrum shown is the average of two individual scans.

## Computational modelling study

Molecular modelling and generation of ligand interaction diagram were carried out using the MOE (Molecular Operating Environment) software package. DNA duplexes containing <sup>diox</sup>T were constructed and minimized with amber force field parameters including Generalized Born implicit solvent model and convergence criteria having an RMS gradient of less than 0.001 kcal mol<sup>-1</sup> Å. For energy minimization water molecules were added to produce distance of 10 Å from the solute to droplet sphere boundaries and sodium counter ions were added to neutralize the system.

Calculation of energy level of <sup>diox</sup>T and four natural bases

Calculations were carried out under B3LYP density functional method and 6-31G\* bases set. HOMO energy of each nucleobase calculated by DFT (B3LYP/6-31G\*) at the optimized geometry by Spartan '16 program. A = 9-methyladenine, T = 1-methylthymine, G = 9-methylguanine, C = 1-methylcytosine.

## Acknowledgements

The authors express sincere thanks for a Grant-in-Aid Priority Research from Japan Society for the Promotion of Science (JSPS). We also thank KAKENHI program (Grant-in-Aid for scientific research C) and Toyota Riken Scholar program for support to S. P. We like to thank Karin Nishimura (Graduate School of Engineering, Kyoto University) for technical assistance to measure mass spectra of synthetic compounds.

## Keywords: DNA, Fluorescent nucleoside, Thymine, SNP typing

- [1] J. N. Wilson and E. T. Kool, *Org. Biomol. Chem.* **2006**, *4*, 4265–4274.
- [2] L. M. Wilhelmsson, *Q. Rev. Biophys.* **2010**, *43*, 159–183.
- [3] R. W. Sinkeldam, N. J. Greco and Y. Tor, *Chem. Rev.* **2010**, *110*, 2579–2619.
- [4] A. Okamoto, K. Tainaka and I. Saito, *J. Am. Chem. Soc.* **2003**, *125*, 4972–4973.
- [5] A. Okamoto, K. Tanaka, T. Fukuta and I. Saito, *J. Am. Chem. Soc.* **2003**, *125*, 9296–9297.
- [6] F. Godde, J. Toulmé and S. Moreau, *Nucleic Acids Res.* **2000**, *28*, 2977–2985.
- [7] R. Tashiro and H. Sugiyama, *J. Am. Chem. Soc.* **2005**, *127*, 2094–2097.
- [8] S.A. Benner, *Acc. Chem. Res.* **2004**, *37*, 784–797.
- [9] A.T. Krueger and E.T. Kool, *Curr. Opin. Chem. Biol.* **2007**, *11*, 588–594.
- [10] I. Hirao, M. Kimoto and R. Yamashige, *Acc. Chem. Res.* **2012**, *45*, 2055–2065.
- [11] J.A. Secrist, J.R. Barrio and N.J. Leonard, *Science*, **1972**, *175*, 646–647.
- [12] L. Sun, M. Wang, E.T. Kool and J. Taylor, *Biochemistry*, **2000**, *39*, 14603–14610.
- [13] A.A. Henry and F.E. Romesberg, *Curr. Opin. Chem. Biol.* **2003**, *7*, 727–733.
- [14] D. Shin, R. W. Sinkeldam and Y. Tor, *J. Am. Chem. Soc.* **2011**, *133*, 14912–14915.
- [15] S.G. Srivatsan, N.J. Greco and Y. Tor, *Angew. Chem., Int. Ed.* **2008**, *47*, 6661–6665.
- [16] R. W. Sinkeldam, L. S. McCoy, D. Shin and Y. Tor, *Angew. Chem., Int. Ed.*, **2013**, *52*, 14026–14030.
- [17] M. Sholokh, R. Sharma, D. Shin, R. Das, O. A. Zaporozhets, Y. Tor and Y. Mély, (2015), *J. Am. Chem. Soc.* **2015**, *137*, 3185–3188.
- [18] S. Park, H. Otomo, L. Zheng and H. Sugiyama, *Chem. Commun.* **2014**, *50*, 1573–1575.
- [19] H. Otomo, S. Park, S. Yamamoto and H. Sugiyama, *RSC Adv.*, **2014**, *4*, 31341–31344.
- [20] I. Okamura, S. Park, R. Hiraga, S. Yamamoto and H. Sugiyama, *Chem. Lett.* **2016**, *46*, 245–248.
- [21] J. H. Han, S. Yamamoto, S. Park and H. Sugiyama, *Chem. Eur. J.* **2017**, *23*, 7607–7613.
- [22] J. H. Han, S. Park, F. Hashiya and H. Sugiyama, *Chem. Eur. J.* **2018**, *64*, 17091–17095.
- [23] Y. Xie, T. Maxson, Y. Tor *J. Am. Chem. Soc.* **2010**, *132*, 11896–11897.
- [24] Y. Xie, T. Maxson, Y. Tor *Org. Biomol. Chem.* **2010**, *8*, 5053–5055.
- [25] G. Mata, N. W. Luedtke *Org. Lett.* **2013**, *15*, 2462–2465.
- [26] G. Mata, N. W. Luedtke *J. Am. Chem. Soc.* **2015**, *137*, 699–707.

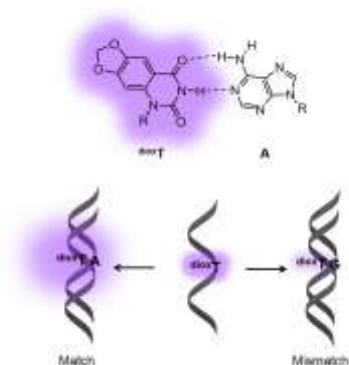
## FULL PAPER

- [27] G. Mata, O. P. Schmidt, N. W. Luedtke *Chem. Commun.* **2016**, 52, 4718–4721.
- [28] S. Yokota, M. Kitahara and K. Nagata, *Cancer Res.* **2000**, 60, 2942–2948.
- [29] M. Himaja, K. Vandana, A. Ranjitha, M. Ramana and A. Karigar, *Int. Res. J. Pharm.* **2011**, 2, 57–61.
- [30] D. Chen, J. Cai, J. Cheng, C. Jing, J. Yin, J. Jiang, Z. Peng and X. Hao, *Sci. Rep.* **2015**, 5, 14972.
- [31] S. Grasso, N. Micale, A. Monforte, P. Monforte, S. Polimeni and M. Zappala, *Eur. J. Med. Chem.* **2000**, 35, 1115–1119.
- [32] M. Suzuki, Y. Nishida, Y. Ohguro, Y. Miura, A. Tsuchida and K. Kobayashi, *Tetrahedron*, **2004**, 15, 159–165.
- [33] N. Srimongkolpithak, S. Sundriyal, F. Li, M. Vedadi and M. J. Fuchter, *MedChemComm*, **2014**, 5, 1821–1828.
- [34] Y. G. Teng, W. T. Berger, N. M. Nesbitt, K. Kumar, T. E. Balius, R. C. Rizzo, P. J. Tonge and I. Ojima, *Bioorg. Med. Chem.* **2015**, 23, 5489–5495.
- [35] F. Godde, J. Toulmé and S. Moreau, *Biochemistry*, **1998**, 37, 13765–13775.
- [36] J. M. Jean and K. B. Hall, *Proc. Natl. Acad. Sci. U.S.A.*, **2001**, 98, 37–41.
- [37] J. N. Wilson, Y. Cho, S. Tan, A. Cuppoletti and E. T. Kool, *ChemBioChem*, **2008**, 9, 279–285.
- [38] C. P. Lawson, A. F. Fuchtbauer, M. S. Wranne, T. Giraud, T. Floyd, B. Dumat, N. K. Andersen, A. H. El-Sagheer, T. Brown and H. Gradén, *Sci. Rep.*, **2018**, 8, 13970.
- [39] A. Dierckx, F. Miannay, N. Ben Gaied, S. Preus, M. Björck, T. Brown, L. M. Wilhelmsson, *Chem. Eur. J.* **2012**, 18, 5987–5997.
- [40] D. D. Burns, K. L. Teppang, R. W. Lee, M. E. Lokensgard and B. W. Purse, *J. Am. Chem. Soc.* **2017**, 139, 1372–1375.
- [41] A. Dumas and N. W. Luedtke, *ChemBioChem*, **2011**, 12, 2044–2051.
- [42] M. Merkel, L. Dehmel, N. P. Ernsting and H. Wagenknecht, *Angew. Chem. Int. Ed.* **2017**, 56, 384–388.
- [43] A. Vignal, D. Milan, M. SanCristobal and A. Eggen, *Genet. Sel. Evol.*, **2002**, 34, 275–305.
- [44] B. obrino, M. Brion and A. Carracedo, *Forensic Sci. Int.* **2005**, 154, 181–194.
- [45] C. Dueymes, J. L. Décout, P. Peltié and M. Fontecave, *Angew. Chem. Int. Ed.* **2002**, 41, 486–489.
- [46] M. E. Hawkins and F. M. Balis, *Nucleic Acids Res.* **2004**, 32, e62.
- [47] M. Hattori, T. Ohki, E. Yanase and Y. Ueno, *Bioorg. Med. Chem. Lett.* **2012**, 22, 253–257.
- [48] A. Okamoto, K. Tainaka and I. Saito, *Tet. Lett.* **2003**, 44, 6871–6874.
- [49] M.S. Wranne, A.F. Fuchtbauer, B. Dumat, M. Bood, A. H. El-Sagheer, T. Brown, H. Gradén, M. Grøtli and L. M. Wilhelmsson, *J. Am. Chem. Soc.* **2017**, 139, 9271–9280.
- [50] M. Kasha, H. Rawls and M. A. El-Bayoumi, *Pure App. Chem.* **1965**, 11, 371–392.
- [51] K. Datta, N. P. Johnson, G. Villani, A. H. Marcus and P. H. von Hippel, *Nucleic Acids Res.* **2011**, 40, 1191–1202.
- [52] C. P. Lawson, A. F. Fuchtbauer, M. S. Wranne, T. Giraud, T. Floyd, B. Dumat, N. K. Andersen, A. H. El-Sagheer, T. Brown, H. Gradén *Sci. reports* **2018**, 8, 13970.
- [53] M. Bood, A. F. Fuchtbauer, M. S. Wranne, J. J. Ro, S. Sarangamath, A. H. El-Sagheer, D. L. Rupert, R. S. Fisher, S. W. Magennis, A. C. Jones *Chem. Sci.* **2018**, 9, 3494–3502.
- [54] D. Liu, Z. Zhang, H. Zhang, Y. Wang *Chem. Commun.* **2013**, 49, 10001–10003.
- [55] Y. Xie, A. V. Dix, Y. Tor *J. Am. Chem. Soc.* **2009**, 131, 17605–17614.
- [56] R. Clayton, M. L. Davis, W. Li, W. Fraser, C. A. Ramsden, *ARKIVOC.* **2017**, 3, 87–104.

## FULL PAPER

## FULL PAPER

We synthesize a new fluorescent thymine analogue,  $\text{dioxT}$ , and explored its photophysical characterization and application.



S. Hirashima, J. H. Han, H. Tsuno, Y. Tanigaki, S. Park\*, H. Sugiyama\*

Page No. – Page No.

**New Size-expanded Fluorescent Thymine Analogue: Synthesis, Characterization, and Application**